An Experimental and Theoretical Study of NSCl Decomposition in the Presence of Trace Amounts of Water

Zhen Guo,[†] Cunyuan Zhao,[‡] David Lee Phillips,*[,†] Evan G. Robertson,*[,§] and Don McNaughton*[,§]

Department of Chemistry, The University of Hong Kong, Pokfulam Road, Hong Kong, P. R. China, School of Chemistry and Chemical Engineering, Sun Yat-Sen University, Guangzhou 510275, P.R. China, and School of Chemistry, Monash University, Victoria, 3800, Australia

Received: March 20, 2008; Revised Manuscript Received: June 12, 2008

An experimental and density functional theory study of the decomposition reaction of NSCl with water molecule(s) into NH_3 and SO_2 is described. Experiments involving the decomposition of NSCl in the presence of trace amounts of water showed that the formation of both HNSO and SO_2 is faster when the cell and the cell surface are fresh and more likely to be coated in adsorbed water. The density functional theory computational results suggest that the decomposition involves two main steps: reactions **1** NSCl + $n$$H_2O$ → HNSO + (n − 1) H_2O + HCl and **2** HNSO + $n$$H_2O$ → NH_3 + SO_2 + (n − 1)H_2O. The barrier for reaction **1** in which NSCl decomposes to form HNSO becomes substantially lower when the explicit hydrogen bonding of water molecules is considered. The water assisted decomposition reaction mechanism can help account for the experimentally observed conversion of NSCl to produce HNSO in the presence of water. The calculated barrier of reaction **2** (the decomposition of HNSO into NH_3 and SO_2) can also explain the experimental observation of SO_2 bands from the decomposition of NSCl in the presence of water.

Introduction

The properties, chemical reactions, and spectroscopy of sulfur−nitrogen compounds have received much experimental and theoretical attention due to their involvement in reactions of interest in synthetic chemistry and in the environment. These thionitroso compounds (especially those with nitrogen−sulfur double bonds) are known to be very unstable and highly reactive.[1–3] A number of infrared spectroscopic investigations have been carried out on two thionitroso containing molecules using matrix isolation and low resolution gas phase techniques.[4–9] An ab initio molecular orbital study performed at the QCISD (T):6−311G (3df, 2p) level of theory with correction of ZPE (zero point energy) by Nguyen and Flammang showed that neutral NSCl is 77 kJ/mol more stable than Cl−N═S.[10] In addition, the product of NSCl in the presence of trace amounts of water, HNSO, has a nonlinear functional group −N═S═O that has gained interest due to its geometry. A recent theoretical study predicted that on the potential energy surface of the HNSO system, cis-HNSO will be at the global minimum and fourteen isomers are kinetically stable with five of these isomers being experimentally suggested in the gas phase.[11] More recently, Robertson, McNaughton, and co-workers[12,13] measured the high resolution FTIR spectra of NSCl and HNSO in the attempted generation of NSCN and NSSCN using NSCl as a precursor. Previously in a low resolution spectroscopy study the bands at 2224 cm^{-1} and 1374 cm^{-1} were mistakenly assigned to NSCN.[14] Recent experimental studies by Robertson, McNaughton and co-workers failed to obtain the production of NSCN from NSCl vapor and these bands at 2224 cm^{-1} and 1337 cm^{-1} were assigned to N_2O and SO_2 using high resolution FTIR spectroscopy.[12,13] They also observed bands associated with HNSO and SO_2 from the hydrolysis of NSCl when trace quantities of water were present and observed the half-life for conversion of NSCl to HNSO to be a few minutes when the pyrolysis products were isolated in a cell and monitored by rapid survey scan experiments.[12] Here, additional experimental results are given for the decomposition of NSCl in the presence of water and these results indicate that the formation of both HNSO and SO_2 is more rapid when the cell and the cell surface are fresh and more likely to be coated in adsorbed water. We also report density functional theory (DFT) and second-order Moller−Plesset perturbation theory (MP2) calculations to investigate the decomposition of NSCl in the presence of trace amounts of water molecules. We aim to elucidate reaction mechanism(s) that can account for a relatively easy conversion of NSCl in the presence of water to HNSO observed experimentally to take a few minutes of time and to elucidate the reaction mechanisms involved in the decomposition of HNSO by trace amounts of water to form a SO_2 byproduct.

Computational and Experimental Details

Thiazyl chloride (NSCl), was prepared by heating a sample of thiodiazyl dichloride ($S_3N_2Cl_2$) to a temperature of 70 °C. The NSCl(g) evolved was passed through a White cell (8 passes × 0.53 m = optical path 4.24 m), for high FTIR analysis. For high resolution spectroscopy the cell was slowly pumped to prevent buildup of hydrolysis products and to ensure a steady flow of sample, with the pressure maintained at *ca.* 30 Pa. To ascertain the half-life of the NSCl in the cell and to test the conditions for optimum production, spectra were recorded at time intervals with the products isolated in the cell and under flowthrough conditions over 5 h of flow. Spectra were recorded

* Authors to whom correspondence should be addressed. Telephone: 852-2859-2160(DLP); +61 3 99054566(EGR); +61 3 99054525(DM). FAX: 852-2857-1586 (DLP); +61 3 9905 4597 (EGR & DM). E-mail: phillips@hkucc.hku.hk; evan.robertson@sci.monash.edu.au; Don.McNaughton@sci.monash.edu.au.

† The University of Hong Kong.

‡ Sun Yat-Sen University.

§ Monash University.

10.1021/jp802445r CCC: $40.75 © 2008 American Chemical Society
Published on Web 08/20/2008

SCHEME 1

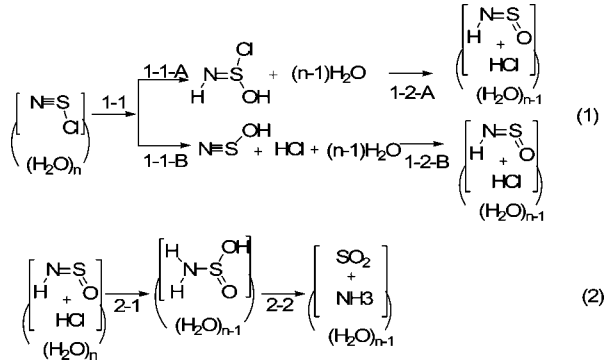

on a Bruker HR120 spectrometer equipped with a liquid nitrogen cooled MCT detector and KBr beamsplitter.

Density functional theory (DFT)[15] and second-order Moller–Plesset perturbation theory (MP2) computations were employed to investigate the decomposition of thiazyl chloride (NSCl) in the presence of water molecules. We have considered two major types of reactions (see Scheme 1). The first reaction type (reaction 1) involves two possible reaction pathways. One is the addition of water to NSCl to produce HNSCl(OH) in water (reaction 1-1-A) followed by the elimination of hydrogen chloride (HCl) in water to produce the simplest sulfinylimide (HNSO) (reaction (1-2-A) as shown below:

$$NSCl + nH_2O \rightarrow HNSCl(OH) + (n-1)H_2O \quad (n = 1, 2, 3) \qquad (1\text{-}1\text{-}A)$$

$$HNSCl(OH) + (n-1)H_2O \rightarrow HNSO + (n-1)H_2O + HCl \qquad (1\text{-}2\text{-}A)$$

These may be added together to obtain the first overall reaction 1 given below:

$$NSCl + nH_2O \rightarrow HNSO + (n-1)H_2O + HCl \qquad (1\text{-}A)$$

The other is the decomposition of NSCl in trace moisture (e.g., in the presence of one or a few water molecules) to hydrogen chloride (HCl) to produce the isomer (NSOH) of HNSO (reaction 1-1-B), and then NSOH transformation to HNSO via an H transfer assisted by water molecule(s) (reaction 1-2-B as shown below:

$$NSCl + nH_2O \rightarrow NSOH + (n-1)H_2O + HCl \qquad (1\text{-}1\text{-}B)$$

$$NSOH + nH_2O \rightarrow HNSO + nH_2O \qquad (1\text{-}2\text{-}B)$$

If we combine the previous two equations, we have

$$NSCl + nH_2O \rightarrow HNSO + (n-1)H_2O + HCl \qquad (1\text{-}B)$$

The second type of reaction is the addition reaction of HNSO with a water molecule to produce $H_2NSO(OH)$ (reaction 2-1) followed by decomposition of $H_2NSO(OH)$ into SO_2 and NH_3 in water (reaction 2-2) as shown below:

$$HNSO + nH_2O \rightarrow H_2NSO(OH) + (n-1)H_2O \quad (n = 1, 2, 3) \qquad (2\text{-}1)$$

$$H_2NSO(OH) + (n-1)H_2O \rightarrow NH_3 + SO_2 + (n-1)H_2O \qquad (2\text{-}2)$$

These two reactions may be added together to obtain the second overall reaction 2 shown below:

$$HNSO + nH_2O \rightarrow NH_3 + SO_2 + (n-1)H_2O \qquad (2)$$

We have considered the effect of water molecules on the reactions by explicitly adding water molecules one by one into the reactant complexes (or water-solvated clusters). The clusters consist of reactants (NSCl) or HNSO molecules and one, two, and three water molecules for reactions 1-1 and 2-1. The reactions 1-2 and 2-2 were only considered with zero, one, or two water molecules.

All of the reactions have been investigated by optimizing the reactant complexes (RC), transition states (TS), and product complexes (PC). These are denoted as $(RC)_{ijn}$, $(TS)_{ijn}$, and $(PC)_{ijn}$ in the following text, tables, and figures, where i represents the number of the reaction, j represents the step of the reaction, and n is the number of water molecules in the reaction. For example, $(RC)_{113}$ represents the reactant complex of the first step of the first reaction with three water molecules, i.e., the reaction complex of $NSCl + 3H_2O \rightarrow HNSCl(OH) + 2H_2O$.

Stationary structures for all of the reactant complexes and transition states and product complexes were fully optimized without a symmetry constraint (e.g., C_1 symmetry) at the B3LYP/aug-cc-pvdz level of theory. Analytical frequency calculations were performed in order to confirm the optimized structure to be either a minimum or a first order saddle point. IRC calculations were performed for all of the reaction systems to confirm the optimized transition state correctly connects the relevant reactants and products. MP2 calculations were also used for reaction 1-1 using the aug-cc-pvdz basis set. Previous work indicates that it is probably necessary to use a basis set including both polarization and diffuse functions for light and heavy atoms in order to obtain a better description of the charge distributions for the charge separated species found in these HCl elimination reactions.[17b]

Results and Discussion

A. Low Resolution and High Resolution FT-IR Spectra of the Decomposition of NSCl. Figure 1 shows the spectra of NSCl in the multipass cell first under flow through conditions where NSCl predominates in the presence of HNSO and second upon isolation of the cell and standing for 3 min. After 3 min, SO_2 is now apparent and HNSO signals have increased markedly at the expense of NSCl. From these experiments it is apparent that the lifetime of NSCl under static conditions in the glass cell is on the order of a few minutes. Figure 2 shows high resolution spectra at the start and finish of a 5 h flowthrough experiment. After 5 h, the intensities of signals from HNSO and SO_2 have decreased markedly with SO_2 showing the greatest decrease. These spectra indicate that the production of both HNSO and SO_2 is more rapid when the cell and the cell surface are fresh and more likely to be coated in adsorbed water. Hence, we surmise that the decomposition of NSCl is assisted by the presence of water through interaction with surface adsorbed water on the ca. 0.25 m^2 borosilicate glass surface and gaseous water desorbed from the surface.

B. Reaction 1: Reactions of NSCl with Water to Produce the Simplest Sulfinylimide HNSO. It has been experimentally shown that HNSO was generated by the reaction of thiazyl chloride (NSCl) with trace moisture in a cell. The conversion of NSCl with water present to HNSO has a half-life of a few minutes. Two possible pathways were examined for the conversion reaction of NSCl to HNSO with water molecules present. The first pathway is the one where NSCl in a trace amount of moisture first undergoes water addition to produce the intermediate HNSCl(OH). Then, the simplest sulfinylimide, HNSO, is formed via the decomposition reaction of

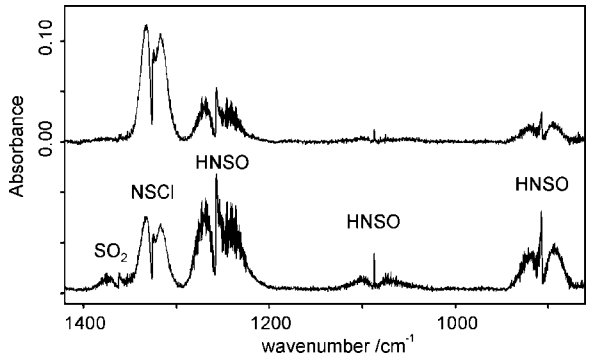

Figure 1. Low resolution (0.4 cm^{-1}) FTIR spectra of NSCl and related byproduct (HNSO and SO_2), with total cell pressure 18 Pa, and path length 4.2 m. Spectra were measured under flowthrough conditions (upper trace), and then 3 min later after the cell had been isolated.

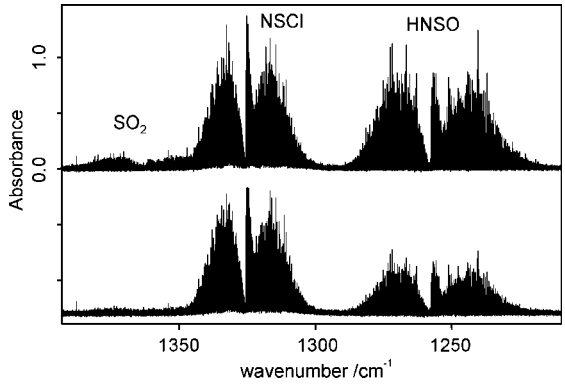

Figure 2. High resolution (0.003 cm^{-1}) FTIR spectra of NSCl and related byproduct measured under flowthrough conditions, with total cell pressure 30 Pa and path length 4.2 m. The upper spectrum was measured first, while the lower spectrum was measured ca. 5 h later when the amount of water in the vacuum system was depleted.

$HNSCl(OH) + (n - 1)H_2O \rightarrow HNSO + (n - 1)(H_2O) + HCl$ (where $n = 1, 2, 3$). The second type of pathway is the decomposition of NSCl in trace moisture (e.g., in the presence of one or a few water molecules) to hydrogen chloride (HCl) and the isomer (NSOH) of HNSO, and then conversion of NSOH to HNSO via an H transfer assisted by water molecule(s).

1-A: Addition of Water Molecule to NSCl and then Decomposition of HNSCl(OH) into HNSO. *1-1-A: NSCl + $nH_2O \rightarrow$ HNSCl(OH) + (n − 1)H_2O (where n = 1, 2, 3).* A DFT investigation of the water assisted addition of NSCl species as a function of the number of water molecules (up to 3) is presented here. The effect of water molecules on the reaction was considered by explicitly adding water molecules one by one into the reactant complex (or water-solvated clusters). Figure 3 depicts simple schematic diagrams of the optimized structures obtained for the $(RC)_{11n}$, $(TS)_{11n}$, and $(PC)_{11n}$ stationary points for the addition reaction that involves one to three water molecules. We also carried out a natural bond order analysis (NBO) to estimate the charges on the atoms of stationary structures reported here, and selected results are given in Table 1. Figure 4 displays the relative energy profiles (in kcal/mol) obtained from the B3LYP/aug-cc-pvdz DFT calculations for the $NSCl + nH_2O \rightarrow HNSCl(OH) + (n - 1)H_2O$ (where $n = 1, 2, 3$) addition reactions.

Inspection of Figure 4 shows that the reaction barriers for the $NSCl + nH_2O \rightarrow HNSCl(OH) + (n - 1)H_2O$ (where $n = 1, 2, 3$) addition reaction are about 48.6 kcal/mol for $n = 1$, 25.7 kcal/mol for $n = 2$, and 18.5 kcal/mol for $n = 3$. The very large reaction barrier, the corresponding small rate constant, and the long lifetime predicted for the addition reaction of $NSCl + H_2O \rightarrow HNSCl(OH)$ suggests the reaction is unlikely to proceed. However, incorporation of an additional water molecule into the reaction dramatically catalyzes the reaction. As seen from Table 2 and Figure 4, the reaction barrier of $(RC)_{112} \rightarrow (TS)_{112}$

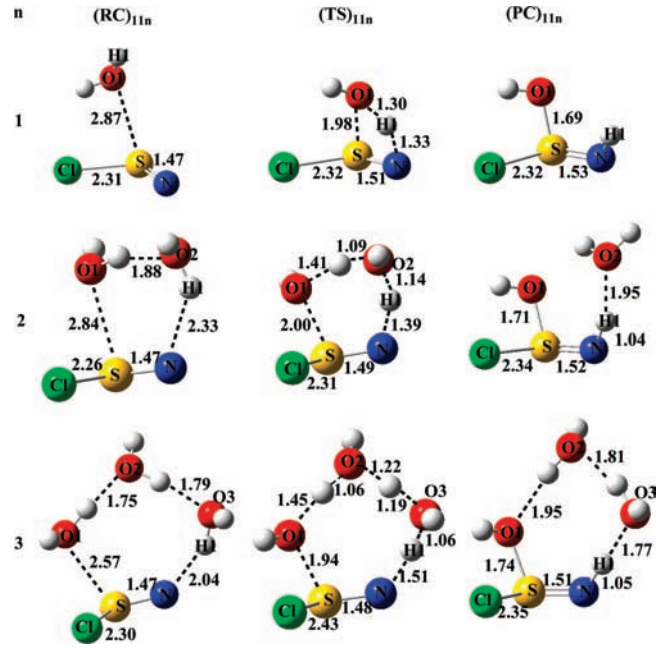

Figure 3. Optimized geometries (bond lengths are in Å) for all the reactants, reactant complexes, transition states, and product complexes obtained from the B3LYP/aug-cc-pvdz calculations are shown for the $NSCl + nH_2O \rightarrow HNSCl(OH) + (n - 1)H_2O$ ($n = 1, 2, 3$) reactions (associated with structures $(RC)_{11n}$, $(TS)_{11n}$, and $(PC)_{11n}$ where $n = 1, 2, 3$).

TABLE 1: NBO Charges on the Selected Atoms for the Reaction $NSCl + nH_2O \rightarrow HNSOCl(OH) + (n - 1)H_2O$ (where $n = 1, 2, 3$)

Species	O1	H1	N	S
$(RC)_{111}$	−0.972	0.493	−0.567	0.970
$(TS)_{111}$	−0.882	0.483	−0.872	1.170
$(PC)_{111}$	−0.882	0.406	−0.947	1.315
$(RC)_{112}$	−0.994	0.504	−0.652	0.993
$(TS)_{112}$	−0.948	0.499	−0.909	1.138
$(PC)_{112}$	−0.906	0.434	−0.938	1.301
$(RC)_{113}$	−0.970	0.513	−0.697	1.030
$(TS)_{113}$	−0.972	0.517	−0.909	1.170
$(PC)_{113}$	−0.928	0.443	−0.932	1.294

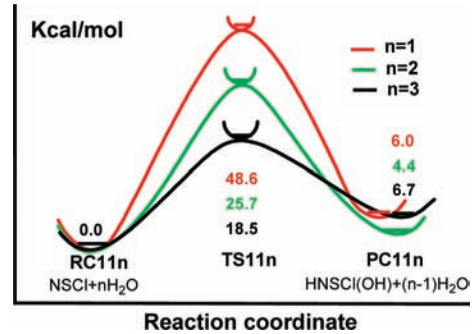

Figure 4. Schematic diagram (not to scale) of the activation free energy profiles (in kcal/mol) obtained from the B3LYP/aug-cc-pvdz DFT calculations for the $(RC)_{11n} \rightarrow (TS)_{11n} \rightarrow (PC)_{11n}$ (where $n = 1, 2, 3$) conversion reactions. See text for more details.

TABLE 2: B3LYP/aug-cc-pvdz Calculated Energies (ΔE) (kcal/mol), Enthalpy (ΔH) (kcal/mol), Free Energies (ΔG) (kcal/mol), Entropy (ΔS) (kcal/mol), Rate Constant (k, s^{-1}), and Half-Life ($t_{1/2}$, s) for Reaction 1 and Reaction 2

Reaction	ΔE [a]	ΔH	ΔG	ΔS	k[b]	$t_{1/2}$[c]
111−113						
111	46.4	44.9	48.6	−0.0124	1.61×10^{-23}	4.3×10^{22}
112	23.2	21.4	25.7	−0.0144	9.76×10^{-7}	7.1×10^{5}
113	15.8	13.8	18.5	−0.0158	1.75×10^{-1}	3.96
120−122						
120	9.1	8.8	8.9	−0.0003	1.90×10^{6}	3.6×10^{-7}
121	3	2.2	3.7	−0.005	1.21×10^{10}	5.7×10^{-11}
122	2.9	1.9	3.4	−0.005	2.02×10^{10}	3.4×10^{-11}
211−213						
211	31.7	30.3	35.8	−0.0184	3.67×10^{-14}	1.9×10^{13}
212	19.3	17.3	22.6	−0.0178	1.75×10^{-4}	4.0×10^{3}
213	17.2	15.1	20.6	−0.0184	5.13×10^{-3}	1.4×10^{2}
220−221						
220	21.6	21.2	22	−0.0027	4.81×10^{-4}	1.5×10^{3}
221	8.9	8	9.8	−0.006	4.11×10^{5}	1.7×10^{-4}

[a] ΔE, ΔH, ΔG, ΔS: Energies of activation with zero point energy, enthalpies, free energies, and entropies of activation for the reaction. [b] k: the rate constant is calculated from the activated free energy by $k = (k_B T/h) \exp(-\Delta G/RT)$. [c] $t_{1/2}$: the half-life is calculated by $t_{1/2} = \ln 2/k$.

→ $(PC)_{112}$ decreases to about half that for the reaction involving only one water molecule. The rate constant is increased by 16 orders of magnitude while the half-life is shortened by 16 orders of magnitude. The significant catalytic effect of the second water molecule can be accounted for by formation of a hydrogen bond between the NSCl molecule and the water hydrogen (H) atom (such as the 2.33 Å distance for the N−H bond in $(RC)_{111}$. Incorporation of three water molecules reduces the reaction barrier of the Gibbs free energy by another 7.2 kcal/mol. Both the rate constant and half-life are changed by another 6 orders of magnitude. This suggests that the hydrogen bonding of the additional water molecules to the NSCl·(H_2O) reactant complex greatly assists the addition process.

In order to better understand this effect, it is useful to compare some structural and charge changes that occur upon going from the reactions that have one water molecule to that where three water molecules are explicitly added to the reaction system. Compared to the reaction system with one water molecule, when the second water molecule is explicitly added to the reaction system there are substantial changes in the structures of the complexes $(RC)_{11n}$, $(TS)_{11n}$, and $(PC)_{11n}$ (where $n = 1, 2$). For instance, the N−H1 bond becomes dramatically stronger and changes its length from 4.34 Å in $(RC)_{111}$ to 2.33 Å in $(RC)_{112}$. As the addition reaction proceeds from the reactants to reach the transition states, $(TS)_{111}$, larger changes in both the structures and atom charges can be observed for the transition state compared to its corresponding reactant complex. For example, the N−H1 bond becomes much stronger and goes from 4.34 Å in $(RC)_{111}$ to 1.33 Å $(TS)_{111}$. These large changes are also accompanied by moderate changes in the O−S bond that becomes stronger and goes from 2.87 Å in $(RC)_{111}$ to 1.98 Å in $(TS)_{111}$. Meanwhile, the N−S bond becomes somewhat weaker and goes from a bond length of 1.47 Å in $(RC)_{111}$ to 1.51 Å in $(TS)_{111}$. These structural changes are also accompanied by noticeable changes in the atom charges. For instance, the charge on the H1 atom decreases significantly from 0.493 in $(RC)_{111}$ to 0.483 in $(TS)_{111}$ as the N−H1 bond begins to form. This is accompanied by noticeable changes in the charges on the N, S, and O1 atoms whose NBO charges go from −0.567, 0.970, and −0.972 in $(RC)_{111}$ to −0.872, 1.170, and −0.882 in $(TS)_{111}$.

Inspection of structures and charges for the $(RC)_{11n} \rightarrow (TS)_{11n} \rightarrow (PC)_{11n}$ (where $n = 1, 2, 3$) addition reaction reveals some trends that appear to correlate with a decrease in the reaction barrier height. For example, the N−H1 bond lengths in the reactants go from 4.33 Å in $(RC)_{111}$ to 2.33 Å in $(RC)_{112}$ and 2.04 Å in $(RC)_{113}$, and the O1−S bond lengths go from 2.87 Å in $(RC)_{111}$ to 2.84 Å in $(RC)_{112}$ and 2.57 Å in $(RC)_{113}$. It is interesting to note that the trends in N−H1 and O−S bond lengths suggest that as the charges of the reaction system in $(RC)_{11n}$ become more shared the barrier for the addition reaction becomes lower. This also correlates with the changes in the N−H1 bond lengths as one goes from $(RC)_{11n}$ to $(TS)_{11n}$ where the differences are about 3.0 Å from $(RC)_{111}$ to $(TS)_{111}$, 0.94 Å from $(RC)_{112}$ to $(TS)_{112}$, and 0.53 Å from $(RC)_{113}$ to $(TS)_{113}$. Similar trends are also seen in the charges of the H1 atom. The preceding trends in the structures of N−H1 and O1−S bonds and the charges of H1 and O1 atoms associated with going from the $(RC)_{11n}$ to their respective $(TS)_{11n}$ suggest less energy is needed to change the structure and charge distribution of the main addition coordinate to approach the transition state as the number of water molecules increases from one to three in the reaction system. This is consistent with the barrier height decreasing from 48.6 kcal/mol for $n = 1$ to 25.7 kcal/mol for $n = 2$ and to 18.5 kcal/mol for $n = 3$ for the $(RC)_{11n} \rightarrow (TS)_{11n} \rightarrow (PC)_{11n}$ (where $n = 1, 2, 3$) addition reactions. We note similar trends for a number of water assisted dehalogenation reactions involving isopolyhalomethanes, halogenated methanols, and halogenated formaldehyde molecules[16–18] (i.e., smaller changes in the key structural features and atom charges as one goes from the reactant complexes to their corresponding transition states when the number of water molecules increases in the water solvated reaction system and a correlation with lower reaction barrier as the number of water molecules increases).

1-2-A: $HNSCl(OH) + nH_2O = HNSO + HCl + nH_2O$ (where $n = 0, 1, 2$). Figure 5 displays the optimized geometries found for the reactions of $HNSCl(OH) + (n-1)H_2O \rightarrow HNSO + HCl + (n-1)H_2O$, i.e., $(RC)_{12n} \rightarrow (TS)_{12n} \rightarrow (PC)_{12n}$ (where $n = 0, 1, 2$). Examination of Figure 5 shows that the gas homogeneous decomposition reaction of $HNSCl(OH) \rightarrow HNSO + HCl$ proceeds through the four centered cyclic transition state $(TS)_{121}$ where the Cl atom is almost detached from the sulfur atom (the S−Cl bond elongates from 2.32 Å to 2.85 Å) and approaches the hydrogen atom in the HNSOCl(OH) H−O bond (the H−Cl distance goes from 2.51 Å in $(RC)_{120}$ to 1.64 Å in $(TS)_{120}$ and the HCl molecule is partially formed in the $(TS)_{120}$). The four-centered transition state is similar to that proposed by Wallington and co-workers[19] in the gas-homogeneous decomposition reaction of $CCl_3(OH) \rightarrow HCl + Cl_2CO$ and also similar to our previous study of the reaction of $CH_2Cl(OH) \rightarrow HCl + HClO$.[17b] In the one and two water-catalytic reactions, the water molecules are incorporated into the leaving group H···Cl through cyclic hydrogen bonds for $(RC)_{12n}$, $(TS)_{12n}$, and $(PC)_{12n}$ ($n = 1, 2$). It is worth noting that there exist systematic changes in going from the reactant complex to the corresponding transition states and product complexes for $(RC)_{12n} \rightarrow (TS)_{12n} \rightarrow (PC)_{12n}$ where $n = 0, 1, 2$. For instance, the H1−O and the S−Cl bonds become systematically elongated for the reactant complexes $(RC)_{12n}$ as the number of water molecules (n) increases from 0 to 2. More linear H-bonds are possible, and they are further strengthened by cooperative effects. Meanwhile,

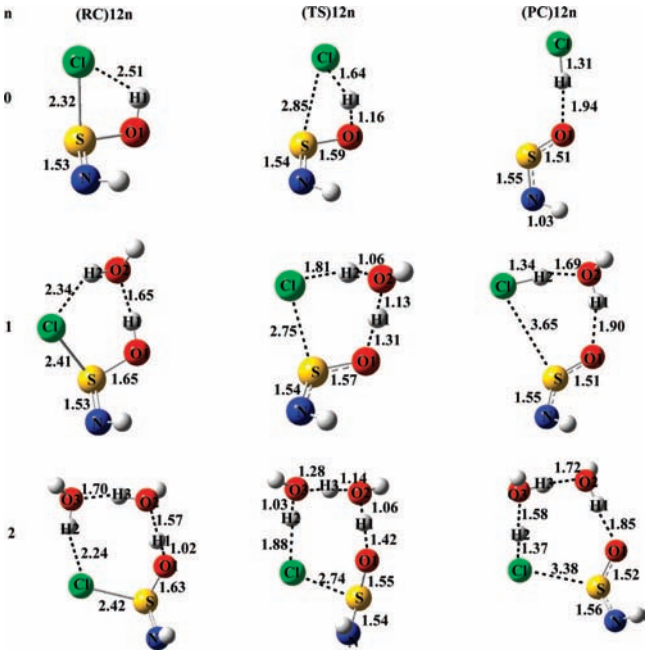

Figure 5. The optimized geometry (bond lengths are in Å) for all of the reactants, reactant complexes, transition states, and product complexes obtained from the B3LYP/aug-cc-pvdz calculations are shown for the HNSCl(OH) + $nH_2O \rightarrow$ HNSO + HCl + nH_2O ($n = 0$, 1, 2) reactions (associated with structures $(RC)_{12n}$, $(TS)_{12n}$, and $(PC)_{12n}$ where $n = 0$, 1, 2).

the distances of the leaving group H···Cl become shorter. The systematic elongation of the S−Cl bonds and the shortening of weak H−Cl interactions for the reactant complexes suggest there is a systematic trend for activating the S−Cl bonds and partial formation of the H−Cl leaving group as more water molecules are explicitly incorporated into the reaction systems.

The H1−O bonds become elongated to 1.16 Å for $(TS)_{120}$, 1.31 Å for $(TS)_{121}$, and 1.42 Å for $(TS)_{122}$, and this indicates that the $H_3O^+Cl^-$ or $H_5O_2^+Cl^-$ ions become almost formed in the transition states $(TS)_{121}$ and $(TS)_{122}$. The transition states $(TS)_{121}$ and $(TS)_{122}$ are greatly stabilized by the $H_3O^+Cl^-$ or $H_5O_2^+Cl^-$ pairs, in which the S···Cl interactions are stronger than those without the water molecule assistance (e.g., smaller S···Cl distances than that without a water molecule present). However, in the product complexes $(PC)_{120}$, $(PC)_{121}$, and $(PC)_{122}$, the zwitterions $H_3O^+Cl^-$ or $H_5O_2^+Cl^-$ will collapse and associate to produce HCl and H_2O molecules.

Examination of the reaction barriers of reaction 1-1 $(RC)_{113} \rightarrow (TS)_{113} \rightarrow (PC)_{113}$ in Figure 4 and reaction 1-2 $(RC)_{122} \rightarrow (TS)_{122} \rightarrow (PC)_{122}$ in Figure 6 shows that the activation free energy of reaction 1-1 is about 15.1 kcal/mol higher than that of reaction 1-2. This indicates that reaction 1-1 is the rate-determining step in the water assisted reactions of NSCl to produce the simplest sulfinylimide HNSO. The energies of the stationary structures for reaction 1-1 were also optimized at the MP2 level of theory using the aug-cc-pvdz basis set and gave similar results to those from the DFT calculations.

1-B: Conversion of NSCl into NSOH and Subsequent Tautomerizations of NSOH and HNSO. Optimized geometries (bond lengths are in Å) for all the reactants, reactant complexes, transition states, and product complexes obtained from the B3LYP/aug-cc-pvdz calculations are shown in Figure 1S of the Supporting Information for the NSCl + $nH_2O \rightarrow$ NSOH + $(n - 1)H_2O$ + HCl ($n = 1$, 2, 3) reactions and NSOH + $nH_2O \rightarrow$ HNSO + nH_2O ($n = 0$, 1, 2)

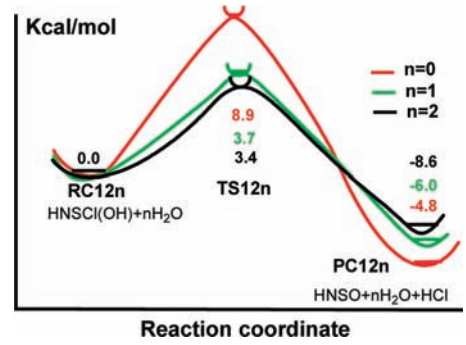

Figure 6. Schematic diagram (not to scale) of the activation free energy profiles (in kcal/mol) obtained from the B3LYP/aug-cc-pvdz calculations for the $(RC)_{12n} \rightarrow (TS)_{12n} \rightarrow (PC)_{11n}$ (where $n = 0$, 1, 2) conversion reactions. See text for more details.

(associated with structures $(RC)_{11n}$, $(TS)_{11n}$, and $(PC)_{11n}$. Due to the similarities of reaction 1-B with reaction 1-A under explicit addition of water molecules, a brief discussion for reaction 1-B is presented here. The calculated results indicate that the reaction barriers (reaction 1-1-B) for the NSCl + $nH_2O \rightarrow$ NSOH + $(n - 1)H_2O$ + HCl (where $n = 1$, 2, 3) conversion reaction are about 19.1 kcal/mol for $n = 1$, 16.7 kcal/mol for $n = 2$, and 13.6 kcal/mol. This suggests water molecules also play an important role in decreasing the reaction barriers of conversion except that the water cluster has a more moderate effect on reaction 1-1-B compared to that of addition (reaction 1-1-A). As for the reaction 1-2-B, NSOH + $n(H_2O) \rightarrow$ HNSO + nH_2O (where $n = 0$, 1, 2), the tautomerization barriers of NSOH and HNSO are calculated to be 34.9 kcal/mol, 10.3 kcal/mol, and 7.7 kcal/mol upon going from the reactions that have zero water molecules to those where two water molecules are explicitly added to the reaction system. Examination of the energy diagram (shown in Figure 2S of the Supporting Information) of reaction 1-B shows that the reaction rate is determined by two steps (conversion and tautomerization). The total barrier of reaction 1-B (calculated from reactions when three water molecules were added into the reaction system) is also 18.5 kcal/mol which is about that of reaction 1-A.

In view of the energetics, reactions 1-A and 1-B are competing in the gas phase and may all be operative in the conversion of NSCl to HNSO. Furthermore, these moderate reaction barriers (18.5 kcal/mol) are also in reasonable agreement with our experimental observation that the half-life of NSCl to HNSO is several minutes in the presence of trace amounts of moisture.

C. Decomposition Reactions of Thionylimide (HNSO) to Produce NH_3 and SO_2 in the Presence of Water. The experimental studies outlined in a previous section show bands of the byproduct HNSO and SO_2. Here we employed density functional theory calculations to investigate the reaction mechanism of HNSO with trace quantities of water to hopefully provide a reasonable explanation for the experimental observations shown in Figures 1 and 2.

$$HNSO + nH_2O \rightarrow H_2NSO(OH) + (n-1)H_2O \quad (\text{where } n = 1, 2, 3) \quad (2\text{-}1)$$

First, we present the addition reaction of water molecules with HNSO to produce the $H_2NSO(OH)$ species. Figures 7 and 8 display the optimized structures and energy diagrams for the reactions $(RC)_{21n} \rightarrow (TC)_{21n} \rightarrow (PC)_{21n}$ where $n = 1$, 2, 3. Analogous to the addition reactions of $(RC)_{11n} \rightarrow (TS)_{11n} \rightarrow (PC)_{11n}$ where $n = 1$, 2, 3, the structures for $(RC)_{21n}$,

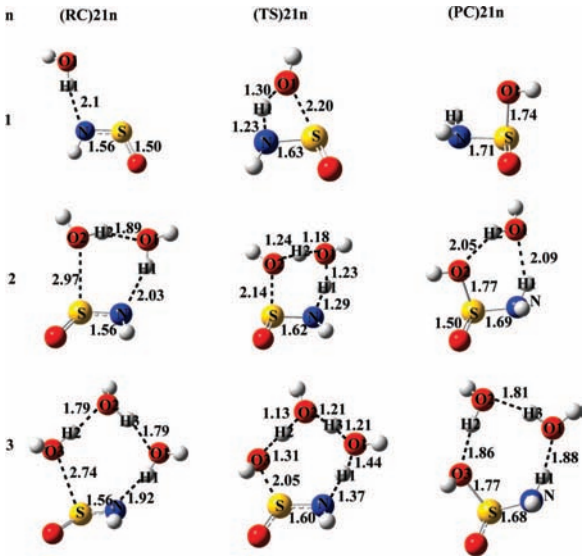

Figure 7. The optimized geometry (bond lengths are in Å) for all of the reactants, reactant complexes, transition states, and product complexes obtained from the B3LYP/aug-cc-pvdz calculations are shown for the $H_2NSO + nH_2O \rightarrow H_2NSO(OH) + (n-1)H_2O$ ($n = 1$, 2, 3) reactions (associated with structures $(RC)_{21n}$, $(TS)_{21n}$, and $(PC)_{21n}$ where $n = 1$, 2, 3).

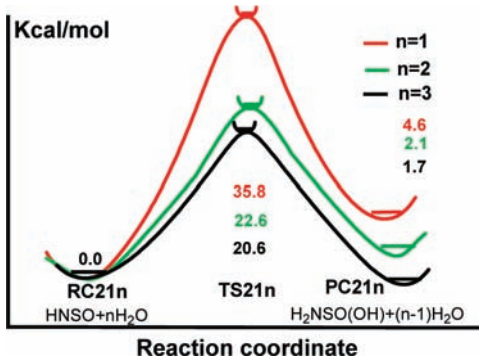

Figure 8. Schematic diagram (not to scale) of the activation free energy profiles (in kcal/mol) obtained from the B3LYP/aug-cc-pvdz calculations for the $(RC)_{21n} \rightarrow (TS)_{21n} \rightarrow (PC)_{21n}$ (where $n = 1$, 2, 3) conversion reactions. See text for more details.

$(TC)_{21n}$, and $(PC)_{21n}$ are quite similar to those of the NSCl addition reactions with water molecules. Examination of Table 2 and Figure 8 shows that the addition reaction has activation free energy barriers of 35.8 kcal/mol for $n = 1$, 22.6 kcal/mol for $n = 2$, and 20.6 kcal/mol for $n = 3$.

Although the main qualitative difference is that reaction 2-1 with the same number of water molecules is faster than reaction 1-1, it is still hard to compare the predicted activation data with the experimental data. As mentioned above, water molecules can noticeably reduce the reaction barrier and accelerate the reaction. As shown in Table 2, the one water molecule reaction has a high reaction barrier, while the second water molecule addition has a significant effect on the reaction of HNSO leading to a decrease in the reaction barrier by 13.2 kcal/mol. However, the addition reaction barrier of reaction 2-1 is only moderately affected (by 2.0 kcal/mol) when the third water molecule is added to the reaction system. The calculated reaction barriers are 22.6 and 20.6 kcal/mol at the B3LYP/aug-cc-pvdz level of theory for the two and three water reaction systems, respectively. Therefore, the gas-phase reaction of 2-1 can probably be reasonably modeled by reactions involving two or three water molecules.

$$H_2NSO(OH) + nH_2O \rightarrow NH_3 + SO_2 + nH_2O \quad (\text{where } n = 0, 1) \quad (2\text{-}2)$$

The decomposition reaction of $H_2NSO(OH)$ to produce NH_3 and SO_2 in the presence of the moisture in air was demonstrated experimentally here and in previous work.[12,13] Decomposition of $H_2NSO(OH)$ into NH_3 and SO_2 in trace quantities of water can be modeled as shown in Figures 9 and 10, namely, $H_2NSO(OH) + nH_2O \rightarrow NH_3 + SO_2 + nH_2O$ or $(RC)_{22n} \rightarrow (TS)_{22n} \rightarrow (PC)_{22n}$ where $n = 0$, 1. The reaction $(RC)_{220} \rightarrow (TS)_{220} \rightarrow (PC)_{220}$ undergoes a similar four-centered cyclic transition state $(TS)_{220}$ to produce NH_3 and SO_2 product. In our water incorporated reactions, the $(RC)_{221}$, $(TS)_{221}$, and $(PC)_{221}$ are structurally similar to the corresponding ones found in the decomposition of HNSCl(OH). It is shown in Table 2 that the reaction barrier without water molecules for the decomposition reaction of HNSO into NH_3 and SO_2 is predicted to be 22.6 kcal/mol at the B3LYP/aug-cc-pvdz level of theory. Analogous to the cases of reactions 1-1, 1-2, and 2-1, the activation energy (E), the activation enthalpies (H), and the activation Gibbs free energy for reaction 2-2 decreased to be 8.9, 8.0, and 9.8 kcal/mol, respectively, when the second water molecule is added to the reaction system.

Considering that reaction 2-2 with two water molecules has a lower reaction barrier (9.8 kcal/mol) than that of reaction 2-1, we believe that for the decomposition of HSNO into NH_3 and SO_2, reaction 2-1 is the rate-determining step. The reaction barriers for reactions 2-2 and 2-1 appear to have reasonable

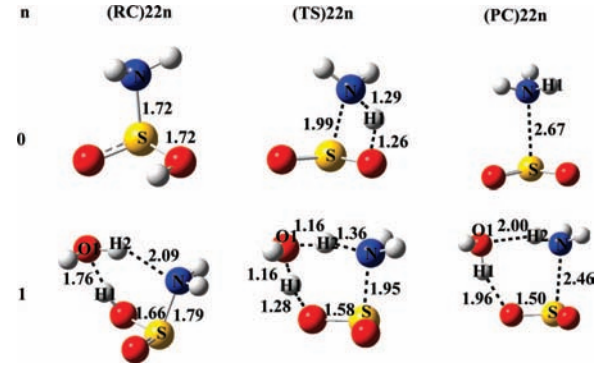

Figure 9. The optimized geometry (bond lengths are in Å) for all of the reactants, reactant complexes, transition states, and product complexes obtained from the B3LYP/aug-cc-pvdz calculations are shown for the $H_2NSOl(OH) + nH_2O \rightarrow NH_3 + SO_2 + nH_2O$ ($n = 0$, 1) reactions (associated with structures $(RC)_{22n}$, $(TS)_{22n}$, and $(PC)_{22n}$ where $n = 0$, 1). See text for more details.

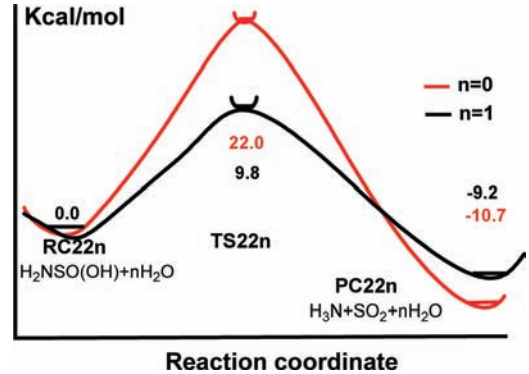

Figure 10. Schematic diagram (not to scale) of the activation free energy profiles (in kcal/mol) obtained from the B3LYP/aug-cc-pvdz calculations for the $(RC)_{22n} \rightarrow (TS)_{22n} \rightarrow (PC)_{22n}$ (where $n = 0$, 1) conversion reactions. See text for more details.

agreement with the experimental observations of the band at 1374 cm^{-1}, belonging to SO_2.[12]

D. Discussion of Results. It is necessary to assemble several water molecules for the water assisted reactions to occur and in some cases water is also a necessary reactant molecule. Since reaction 1-1 is the rate-determining step in the water reactions of NSCl to produce the simplest sulfinylimine HNSO, we have not considered the contribution of reaction 1-2 to the reaction rate in this system and focus on reaction 1-1 to make a rough comparison between the predicted kinetics and experimental observations of the NSCl lifetime. Examination of Table 2 shows the rate constants of the $NSCl(H_2O)_n$ reactant complexes to form the product complexes (e.g., $(RC)_{11n} \rightarrow (TS)_{11n} \rightarrow (PC)_{11n}$) were estimated to be 1.61×10^{-23} s^{-1} for $n = 1$, 9.76×10^{-7} s^{-1} for $n = 2$, and 1.75×10^{-1} s^{-1} for $n = 3$ and predicted lifetimes for the $NSCl(H_2O)_n$ reactant complexes of 4.3×10^{22} s for $n = 1$, 7.1×10^5 s for $n = 2$, and 3.96 s for $n = 3$. These results indicate that a simple gas phase reaction of NSCl with one H_2O molecule cannot explain the observed experimental lifetime of several minutes for NSCl in the presence of trace amounts of water in the reaction chamber and that two or more water molecules are needed to convert the NSCl to HNSO on a time scale comparable to experimental observations.

At low vapor pressure and room temperature conditions, water clusters will have very low concentrations in the gas phase and purely gas phase reactions of NSCl with water clusters may not fully account for the relatively fast conversion of NSCl to HSNO or the further decomposition of HSNO to a SO_2 byproduct as observed in the FT-IR experiments (see Figures 1 and 2 and references[12] and[13]). However, it is worth noting that water has a strong preference for attachment to the walls of containers like glass, Pyrex, and metals, and wall effect reactions may be implicated in the production of the observed byproduct. Indeed, experimental observations in the Monash laboratories over a number of years have shown that the pressure buildup and drop in an isolated glass cell is at least partly associated with water molecules and highly dependent on the pretreatment of the cell. It is conceivable that a few dangling OH bonds of bound water molecules at the borosilicate surface of the container would be able to effectively mimic a water cluster and efficiently react with NSCl to convert it to HSNO in a few minutes and also to react with HSNO to make a SO_2 byproduct as seen in the experiments. These types of water assisted reactions are consistent with our present theoretical results and appear reasonably consistent with the experimental observations and conditions. It would be interesting to better characterize the decomposition reactions of NSCl and HSNO as a function of container size and cell pretreatment through baking or water saturation in order to explore how much these wall effect reactions may contribute to the overall decomposition reactions observed experimentally.

Conclusions

In our FTIR spectra, we observe bands associated with HNSO and SO_2 from hydrolysis with trace quantities of water. The half-life for conversion of NSCl to HNSO was observed to be a few minutes when the pyrolysis products were isolated in the cell and monitored by rapid survey scans. A density functional theory study of the reactions of NSCl and HSNO with water was presented in which hydrogen bonded water molecules (up to 3) were explicitly included in the reaction systems. The calculations show that the conversion reactions of NSCl and decomposition reactions of HNSO are significantly influenced by hydrogen bonding effects which are enhanced as the number of water molecules increases. The conversion reaction of NSCl includes two competing reaction pathways: reaction 1-A and reaction 1-B. The calculated results show that 1-1-A is rate-determining in the pathway 1-A. However, the total reaction rate in reaction 1-B is determined by two steps (reaction 1-1-B and reaction 1-2-B). It is worth noting that the reaction barriers of reactions 1-A and 1-B are quite similar and both can possibly be used to explain the experimental observation of a few minutes half-time of conversion of NSCl to HNSO in the presence of trace amounts of moisture. The decomposition reaction of HNSO involves two parts: reaction 2-1 and reaction 2-2. The overall decomposition reaction barrier (20.6 kcal/mol obtained from the B3LYP/aug-cc-pvdz calculations) of the rate-determining step reaction 2-1 can help explain the experimental observation of SO_2 formation of from hydrolysis due to the presence of trace quantities of water.

Acknowledgment. This research has been supported by grants from the Research Grants Council of Hong Kong (HKU 7036/04P), the award of a Croucher Foundation Senior Research Fellowship (2006−07) from the Croucher Foundation, and an Outstanding Researcher Award (2006) from the University of Hong Kong to D.L.P., E.G.R., and D.McN. thank the Australian Research Council for support and Finlay Shanks for essential instrument support.

Supporting Information Available: The optimized geometries for all of the reactants, reactant complexes, transition states, and product complexes obtained from the B3LYP/aug-cc-pvdz calculations are shown for the reactions: $NSCl + nH_2O \rightarrow HNSCl(OH) + (n-1)H_2O$ ($n = 1, 2, 3$); $HNSCl(OH) + (n-1)H_2O \rightarrow HNSO + (n-1)H_2O + HCl$ ($n = 1, 2, 3$); $HNSO + n(H_2O) \rightarrow H_2NSO(OH) + (n-1)H_2O$ ($n = 1, 2, 3$); $NSCl + nH_2O \rightarrow NSOH + (n-1)H_2O + HCl$; $NSOH + nH_2O \rightarrow HNSO + nH_2O$; $H_2NSO(OH) + (n-1)(H_2O) \rightarrow NH_3 + SO_2 + (n-1)(H_2O)$ ($n = 1, 2$). The energy diagram of conversion NSCl to HNSO under three water molecules is also collected. This material is available free of charge via the Internet at http://pubs.acs.org.

References and Notes

(1) Middleton, W. J. *J. Am. Chem. Soc.* **1966**, *88*, 3842.

(2) Bryce, M. R.; Taylor, P. C. *J. Chem. Soc., Perkin Trans I* **1990**, 3225.

(3) Takahashi, M.; Okasaki, R.; Inamoto, N.; Sugarawa, T.; Inamura, H. *J. Am. Chem. Soc.* **1992**, *114*, 1830.

(4) Miller, K. V.; Emken, W. C.; Duncan, L. C. *J. Fluorine Chem.* **1984**, *26*, 125.

(5) Jacox, M. E. *J. Phys. Chem. Ref. Data* **1984**, *13*, 945.

(6) Peake, S. C.; Downs, A. J. *J. Chem. Soc., Dalton Trans.* **1974**, 859.

(7) Glemser, O.; Richert, H. Z. *Anorg. Allg. Chem* **1961**, *307*, 313.

(8) Mirri, A. M.; Guarnieri, A. *Spectrochim. Acta, Part A* **1967**, *23*, 2159.

(9) Muller, A.; Nagarajan, G.; Glemser, O.; Cyvin, S. F.; Wegener, J. *Spectrochim. Acta, Part A* **1967**, *23*, 2683.

(10) Nguyen, M. T.; Flammang, R. *Chem. Ber.* **1996**, *129*, 1379.

(11) Chi, Y. J.; Yu, H. T. *Chin. J. Chem.* **2003**, *21*, 30.

(12) Robertson, E. G.; Thompson, C. D.; Lucie, S.; McNaughton, D. *Phys. Chem. Chem. Phys.* **2005**, *7*, 483.

(13) (a) Puskar, L. P.; Robertson, E. G.; McNaughton, D. *J. Mol. Spectrosc.* **2006**, *240*, 244. (b) Robertson, E. G.; McNaughton, D. *J. Mol. Spectrosc.* **2006**, *238*, 56–63.

(14) (a) Allaf, A. W.; Suffolk, R. J. *J. Chem. Res.* **1994**, *1*, 186. (b) Robertson, E. G.; McNaughton, D. *J. Phys. Chem. A* **2003**, *107*, 642–650.

(15) (a) Beck, A. D. *J. Chem. Phys.* **1993**, *98*, 5648. (b) Becke, A. D. *Phys. Rev. A* **1988**, *38*, 3098. (c) Vosko, S. H.; Wilk, L.; Nusair, M *Can. J. Phys.* **1980**, *58*, 1200. (d) Lee, C.; Yang, W.; Parr, R. G. *Phys. Rev. B* **1988**, *37*, 785.

(16) (a) Kwok, W. M.; Zhao, C.; Guan, X.; Li, Y. L.; Du, Y.; Phillips, D. L. *J. Chem. Phys.* **2004**, *120*, 9017. (b) Lin, X.; Zhao, C.; Phillips, D. L *Chem. Phys. Lett.* **2004**, *397*, 488. (c) Lin, X.; Guan, X.; Kwok, W. M.; Zhao, C.; Du, Y.; Li, Y. L.; Phillips, D. L. *J. Phys. Chem. A* **2005**, *109*, 981.

(17) (a) Li, Y. L.; Zhao, C.; Kwok, W. M.; Guan, X.; Zuo, P.; Phillips, D. L. *J. Chem. Phys.* **2003**, *119*, 4671. (b) Kwok, W. M.; Zhao, C.; Li, Y. L.; Guan, X.; Phillips, D. L. *J. Chem. Phys.* **2004**, *120*, 3323. (c) Phillips, D. L.; Zhao, C.; Wang, D. *J. Phys. Chem. A* **2005**, *109*, 9653.

(18) (a) Kwok, W. M.; Zhao, C.; Li, Y. L.; Guan, X.; Wang, D.; Phillips, D. L. *J. Am. Chem. Soc.* **2004**, *126*, 3119. (b) Zhao, C.; Lin, X.; Kwok, W. M.; Guan, X.; Du, Y.; Wang, D.; Hung, K. F.; Phillips, D. L. *Chem. Eur. J.* **2005**, *11*, 1093.

(19) Wallington, T. J.; Schneider, W. F.; Barnes, I.; Becker, K. H.; Sehested, J.; Nielsen, O. J. *Chem. Phys. Lett.* **2000**, *322*, 97–102.

JP802445R